A Robust Timing Synchronization Design in OFDM Systems–Part II: High-Mobility Cases

Yasamin Mostofi, *Member, IEEE,* and Donald C. Cox, *Fellow, IEEE*

***Abstract*— In this paper we consider the design of a robust timing synchronization algorithm for pilot-aided OFDM systems in high-mobility fading environments. We first analyze the impact of both mobility and timing errors on the performance of a pilot-aided OFDM system for frequency selective fading channels, by deriving an expression for channel estimation error variance. The analysis will show that, even for high levels of mobility, a pilot-aided channel estimator is considerably sensitive to timing errors, due to the impact of rotations in different bases. We then show how this sensitivity can be utilized to design a robust timing synchronization algorithm for mobile OFDM systems, without relying on synchronization training information. Theoretical results are then confirmed by simulating the performance of an OFDM system in high delay and Doppler spread fading environments. Finally, we show how the proposed mathematical framework and algorithm can be used to address timing synchronization in the presence of a frequency offset as well. The analysis of this paper is the extension of the derivations of Part I [8], the accompanying paper on the design of a robust timing synchronizer for low-mobility OFDM systems.**

***Index Terms*— Channel estimation, mobility, orthogonal frequency division multiplexing (OFDM), timing synchronization.**

I. Introduction

RECENTLY, there has been considerable interest in Orthogonal Frequency Division Multiplexing (OFDM) for high-mobility data communication. The use of OFDM for Digital Audio Broadcasting (DAB [5]), Digital Video Broadcasting (DVB [14]) and Digital Video Broadcasting-Handheld (DVB-H [4]) is an evidence of this trend.

Transmission in a mobile communication environment can experience high Doppler spread. This can degrade the performance of an OFDM system by ruining the orthogonality of the sub-carriers [10]. Timing synchronization in an OFDM system will then become more challenging due to the increase in the amount of Inter-Carrier-Interference. Also, in mobile environments there can be sporadic birth and death of the paths, for instance as the vehicle turns around the corner, resulting in timing drifts. Such drifts can happen on the course of several OFDM symbols, depending on the environment, and are typically small. Nevertheless, the drift needs to be corrected after a number of OFDM symbols. Therefore, the algorithm should have a good resolution to track small timing drifts robustly and correct them. Finally, deployment of OFDM systems in Single Frequency Networks[1] (SFN) can result in channels with considerably high delay spread, making the design of a robust timing synchronizer further challenging.

In this paper, we are interested in designing a robust timing synchronization algorithm for high delay and Doppler spread environments, without relying on synchronization training information. In part I, we considered timing synchronization in low-mobility OFDM systems. We showed that pilot-aided channel estimators are considerably sensitive to timing synchronization errors since the equivalent channel rotates in a different base than the estimated equivalent channel. Based on the analysis, we proposed a robust timing synchronizer that exploits this sensitivity, without relying on training information.

In mobile environments, channel time-variations in an OFDM symbol introduce additional Inter-Carrier-Interference (ICI). Then the main goal of this paper is to investigate if the same level of sensitivity exists for high-mobility applications. We first analyze the impact of both mobility and timing synchronization errors on the performance of a pilot-aided channel estimator. We derive analytical expressions for average Signal to Interference Ratio (SIR) and average channel estimation error variance in the presence of timing errors for high-mobility applications. Our mathematical derivations show that a pilot-aided channel estimator is still considerably sensitive to timing errors (due to the impact of rotations in different bases) even for high levels of mobility. We then show how to extend the proposed algorithm of Part I, by exploiting this sensitivity to design a robust timing synchronizer for high Doppler spread environments. The mathematical analysis of this paper is for the general case that channel is time-varying within one OFDM symbol. Since frequency offset can be modeled as a time-variation in the channel, we also show how the mathematical framework of this paper can be utilized to address the impact of timing errors on channel estimation in the presence of both a frequency offset and Doppler. It should be noted that this paper is on designing robust timing synchronization algorithms for high-mobility applications and is not about designing mobility mitigation methods. For more on mobility mitigation in OFDM systems, see [7], [10], [13], [15].

We conclude this section with an overview of the paper. In Section II, we analyze the impact of timing errors on a mobile pilot-aided OFDM system by deriving mathematical expressions for the average Signal to Interference Ratio. In

Manuscript received May 1, 2006; revised December 19, 2006; accepted May 30, 2007. The associate editor coordinating the review of this paper and approving it for publication was C. Tellambura.

Y. Mostofi is with the Department of Electrical and Computer Engineering, University of New Mexico, Albuquerque, NM 87131 USA (e-mail: ymostofi@ece.unm.edu).

D. C. Cox is with the Department of Electrical Engineering, Stanford University, Stanford, CA, 94305 USA (e-mail: dcox@spark.stanford.edu).

Digital Object Identifier 10.1109/TWC.2007.xxxxx.

[1]SFN refers to DAB and DVB type environments in which adjacent base stations transmit in the same frequencies to save the bandwidth.

Section III, we derive analytical expressions for the average channel estimation error variance of a pilot-aided channel estimator in the presence of timing errors and for high-mobility applications. The results of Section III shows that the super-sensitivity of a pilot-aided channel estimator to timing errors can still be exploited to design robust timing synchronization algorithms. In Section IV, we then show how to utilize this sensitivity by extending the algorithm proposed in Part I to high-mobility applications. Section V shows the robust performance of the proposed synchronizer in high delay and Doppler spread environments. In Section VI, we show how the proposed mathematical framework and algorithm can be used for timing synchronization in the presence of a frequency offset and in high delay and Doppler spread environments. We conclude in Section VII.

II. Effect of Timing Synchronization Errors on Mobile OFDM Systems

In high-mobility environments, channel time-variations within one OFDM symbol can not be neglected. Let $h_k^{(i)}$ represent the k^{th} path (multipath component) of the time-varying channel impulse response at time instant $t = i \times T_s$, where T_s is the sampling period. In this paper, we use the same notation of Part I [8] for basic parameters of a pilot-aided OFDM system. A constant channel is assumed over the time interval $i\times T_s \le t < (i+1)\times T_s$ with $t = 0$ indicating the start of the data part of the symbol. Let $\vartheta_{mob,i}$ represent the time-domain channel output for the case of perfect synchronization, in the absence of noise and in a mobile environment. Then,

$$\vartheta_{mob,i} = \sum_{k=0}^{G} h_k^{(i)} x_{((i-k))_N} \quad 0 \le i \le N-1, \qquad (1)$$

where x_k is the time-domain transmitted data point and G is the guard interval length. Let $\Omega_{mob,i}$ represent the FFT of $\vartheta_{mob,i}$. The following can be easily verified (see [10] for details):

$$\Omega_{mob,i} = H_{i,0}X_i + \underbrace{\sum_{z=1}^{N-1} H_{i,z}X_{((i-z))_N}}_{ICI_{mob}(i)} \quad 0 \le i \le N-1, \ (2)$$

where $H_{i,z} = \frac{1}{N}\sum_{g=0}^{C}\sum_{g'=0}^{N-1} h_g^{(g')} e^{-\frac{j2\pi}{N}(z\times(g'-g)+g\times i)}$, X_i denotes the transmitted data point at the i^{th} sub-carrier, C represents the normalized length of the channel delay spread (normalized by the sampling period) as defined in Part I, N is the number of sub-carriers, and ICI_{mob} is the ICI that is caused by mobility.

A. Case of $m > 0$ for Mobile OFDM

Consider a case where an error of m sampling periods to the right side has occurred as described in Section III of Part I. We take timing errors to be bounded by the cyclic prefix in this paper, i.e. $|m| < G$. Then, the terms $\vartheta_{mob,0}, \vartheta_{mob,1}, \ldots, \vartheta_{mob,m-1}$ are missed and instead m data points of the next OFDM symbol are erroneously selected. The received signal will then be as follows:

$$y_{mob,i}^r = \vartheta_{mob,((i+m))_N}\times\gamma_i^r + s_{mob,i} + w_{mob,i}^r \quad 0 \le i \le N-1, \qquad (3)$$

where the superscript r denotes the case of $m > 0$. $\gamma_i^r = \begin{cases} 1 & 0 \le i \le N-m-1 \\ 0 & N-m \le i \le N-1 \end{cases}$, $w_{mob,i}^r$ is a sample of AWGN and $s_{mob,i} = \begin{cases} 0 & 0 \le i \le N-m-1 \\ y_{mob,pf}^{next}(i-N+m) & else \end{cases}$. $y_{mob,pf}^{next}(i)$ represents the i^{th} sample of the output cyclic prefix of the next OFDM symbol (excluding the effect of AWGN) for the mobile case. Using Eq. 2, the FFT of $y_{mob,i}^r$, $Y_{mob,i}^r$, will be as follows:

$$\begin{aligned} Y_{mob,i}^r &= \sum_{k=0}^{N-1}\sum_{k'=0}^{N-1} \frac{\Gamma_k^r}{N} H_{((i-k))_N,k'} X_{((i-k-k'))_N} e^{\frac{j2\pi m(i-k)}{N}} \\ &+ S_{mob,i} + W_{mob,i}^r \quad 0 \le i \le N-1, \end{aligned} \qquad (4)$$

where Γ^r, S_{mob} and W_{mob}^r are the FFTs of γ^r, s_{mob} and w_{mob}^r respectively. The first term on the right hand side of Eq. 4 will be as follows:

$$\begin{aligned} &\textstyle\sum_{k=0}^{N-1}\sum_{k'=0}^{N-1} \frac{\Gamma_k^r}{N} H_{((i-k))_N,k'} X_{((i-k-k'))_N} e^{\frac{j2\pi m(i-k)}{N}} = \\ &\quad \textstyle\sum_{k'=0}^{N-1} \frac{\Gamma_0^r}{N} H_{i,k'} X_{((i-k'))_N} e^{\frac{j2\pi mi}{N}} + \\ &\textstyle\sum_{k=1}^{N-1}\sum_{k'=0}^{N-1} \frac{\Gamma_k^r}{N} H_{((i-k))_N,k'} X_{((i-k-k'))_N} e^{\frac{j2\pi m(i-k)}{N}} = \\ &\quad \frac{\Gamma_0^r}{N} H_{i,0} X_i e^{\frac{j2\pi mi}{N}} + \frac{\Gamma_0^r}{N} e^{\frac{j2\pi mi}{N}} ICI_{mob}(i) + \\ &\textstyle\sum_{k=1}^{N-1}\sum_{k'=0}^{N-1} \frac{\Gamma_k^r}{N} H_{((i-k))_N,k'} X_{((i-k-k'))_N} e^{\frac{j2\pi m(i-k)}{N}} = \\ &\quad \frac{\Gamma_0^r}{N} H_{i,0} X_i e^{\frac{j2\pi mi}{N}} + \frac{\Gamma_0^r}{N} e^{\frac{j2\pi mi}{N}} ICI_{mob}(i) + \\ &\quad \underbrace{\sum_{k=1}^{N-1}\sum_{k'=0}^{N-1}}_{k+k'=N} \frac{\Gamma_k^r}{N} H_{((i-k))_N,k'} X_{((i-k-k'))_N} e^{\frac{j2\pi m(i-k)}{N}} + \\ &\quad \underbrace{\sum_{k=1}^{N-1}\sum_{k'=0}^{N-1}}_{k+k'\neq N} \frac{\Gamma_k^r}{N} H_{((i-k))_N,k'} X_{((i-k-k'))_N} e^{\frac{j2\pi m(i-k)}{N}}. \end{aligned} \qquad (5)$$

Therefore, we will have,

$$\begin{aligned} &\textstyle\sum_{k=0}^{N-1}\sum_{k'=0}^{N-1} \frac{\Gamma_k^r}{N} H_{((i-k))_N,k'} X_{((i-k-k'))_N} e^{\frac{j2\pi m(i-k)}{N}} = \\ &\quad \frac{\Gamma_0^r}{N} H_{i,0} X_i e^{\frac{j2\pi mi}{N}} + \frac{\Gamma_0^r}{N} e^{\frac{j2\pi mi}{N}} ICI_{mob}(i) + \\ &\quad \textstyle\sum_{k=1}^{N-1} \frac{\Gamma_k^r}{N} H_{((i-k))_N,N-k} X_i e^{\frac{j2\pi m(i-k)}{N}} + \\ &\quad \underbrace{\sum_{k=1}^{N-1}\sum_{k'=0}^{N-1}}_{k+k'\neq N} \frac{\Gamma_k^r}{N} H_{((i-k))_N,k'} X_{((i-k-k'))_N} e^{\frac{j2\pi m(i-k)}{N}} = \\ &\quad e^{\frac{j2\pi mi}{N}} H_i^{norot,r} X_i + \frac{\Gamma_0^r}{N} e^{\frac{j2\pi mi}{N}} ICI_{mob}(i) + \\ &\quad \underbrace{\sum_{k=1}^{N-1}\sum_{k'=0}^{N-1}}_{k+k'\neq N} \frac{\Gamma_k^r}{N} H_{((i-k))_N,k'} X_{((i-k-k'))_N} e^{\frac{j2\pi m(i-k)}{N}}, \end{aligned} \qquad (6)$$

where $H_i^{norot,r} = \sum_{z=0}^{N-1} e^{-j\frac{2\pi mz}{N}} \frac{\Gamma_z^r}{N} H_{((i-z))_N,N-z}$ with $H_{i,z} = \frac{1}{N}\sum_{g=0}^{C}\sum_{g'=0}^{N-1} h_g^{(g')} e^{-\frac{j2\pi}{N}(z\times(g'-g)+g\times i)}$. Note that $H_{i,0} = H_{i,N}$. Using this, Eq. 4 can be written as follows for

$0 \leq i \leq N-1$:

$$Y^r_{mob,i} = \underbrace{e^{\frac{j2\pi mi}{N}} H^{norot,r}_i}_{H^r_{mob,eq}(i)} X_i + \underbrace{\frac{\Gamma^r_0}{N} e^{\frac{j2\pi mi}{N}} ICI_{mob}(i)}_{\text{ICI due to mobility}} + \overbrace{\underbrace{\sum_{k=1}^{N-1}\sum_{k'=0}^{N-1}}_{k+k'\neq N} \frac{\Gamma^r_k}{N} H_{((i-k))_N,k'} X_{((i-k-k'))_N} e^{\frac{j2\pi m(i-k)}{N}} + S_{mob,i}}^{I^r_{mob,i}}$$
$$\text{ICI \& ISI due to timing errors} \quad + W^r_{mob,i}. \tag{7}$$

We derive an expression for the average power of the interference terms next. Let the auto-correlation function of the g^{th} channel path be defined as follows: $R_g(z) = E(h^{(g')}_g h^{(g'-z)*}_g)$. Then the normalized auto-correlation function will be: $R_{g,norm}(z) = \frac{R_g(z)}{\sigma^2_g}$, with σ^2_g representing the power of the g^{th} channel path. To make the analysis tractable, we make the assumption that $R_{g,norm}(z)$ is the same for all the channel paths (hence the subscript g will be dropped, i.e. $R_{norm}(z)$). This assumption, however, does not affect final results and conclusions of the paper.

Theorem 1: The average Signal to Interference Ratio for $m > 0$, $SIR^r_{mob,ave} = \frac{E\{|H^{norot,r}_i X_i|^2\}}{E\{|\frac{\Gamma^r_0}{N} e^{\frac{j2\pi mi}{N}} ICI_{mob}(i) + I^r_{mob,i} + S_{mob,i}|^2\}}$, will satisfy the following equation for a mobile OFDM system:

$$\frac{1}{SIR^r_{mob,ave}} = \frac{N^2}{\sum_{g=m}^{N-1}\sum_{g'=m}^{N-1} R_{norm}(g-g')} - 2\frac{\Re\{\sum_{z=0}^{m-1}\sum_{z'=z+1}^{C}\sum_{g'=m}^{N-1}\sigma^2_{z'} R_{norm}(N-m+z-g')\}}{\sigma^2_H \sum_{g=m}^{N-1}\sum_{g'=m}^{N-1} R_{norm}(g-g')} - 1, \tag{8}$$

where $\sigma^2_H = \sum_{i=0}^{C} \sigma^2_{h_i}$ and $\Re\{.\}$ represents the real part of the argument.

Proof: Theorem 1 is proved in the Appendix. ■

B. Case of $m < 0$ for Mobile OFDM

In this case, an error of m sampling periods to the left side has occurred. Then only $d = \max(C-(G+m), 0)$ data points are corrupted due to the interference from the previous symbol. The received signal can thus be written as follows:

$$y^l_{mob,i} = \vartheta_{mob,((i+m))_N} \times \gamma^l_i + \psi_{mob,i} + w^l_{mob,i} \quad 0 \leq i \leq N-1, \tag{9}$$

where $w^l_{mob,i}$ is a sample of AWGN,

$$\gamma^l_i = \begin{cases} 0 & 0 \leq i \leq d-1 \\ 1 & d \leq i \leq N-1 \end{cases} \text{ and}$$

$$\psi_{mob,i} = \begin{cases} y_{mob,pf}(G+m+i) & 0 \leq i \leq d-1 \\ 0 \quad else \end{cases}.$$

$y_{mob,pf}(i)$ represents the i^{th} sample of the output cyclic prefix of the current OFDM symbol (excluding the effect of AWGN) for the mobile case. Similar to the case of $m > 0$, the FFT of $y^l_{mob,i}$ will be as follows for $0 \leq i \leq N-1$:

$$Y^l_{mob,i} = \underbrace{e^{\frac{j2\pi mi}{N}} H^{norot,l}_i}_{H^l_{mob,eq}(i)} X_i + \underbrace{\frac{\Gamma^l_0}{N} e^{\frac{j2\pi mi}{N}} ICI_{mob}(i)}_{\text{ICI due to mobility}} + \overbrace{\underbrace{\sum_{k=1}^{N-1}\sum_{k'=0}^{N-1}}_{k+k'\neq N} \frac{\Gamma^l_k}{N} H_{((i-k))_N,k'} X_{((i-k-k'))_N} e^{\frac{j2\pi m(i-k)}{N}} + \Psi_{mob,i}}^{I^l_{mob,i}}$$
$$\text{ICI \& ISI due to timing errors} \quad + W^l_{mob,i}, \tag{10}$$

where $H^{norot,l}_i = \sum_{z=0}^{N-1} e^{-j\frac{2\pi mz}{N}} \frac{\Gamma^r_z}{N} H_{((i-z))_N,N-z}$, Γ^l, Ψ_{mob} and W^l_{mob} are the FFTs of γ^l, ψ_{mob} and w^l_{mob} respectively. $\Psi_{mob,i} = \sum_{k=0}^{d-1} \psi_{mob,k} e^{-\frac{j2\pi ki}{N}}$ where $\psi_{mob,k}$ can be written as follows:

$$\psi_{mob,k} = \sum_{k'=0}^{G+m+k} h^{(m+k)}_{k'} x_{N+m+k-k'} + \sum_{k'=G+m+k+1}^{C} h^{(m+k)}_{k'} x^{prev}_{N-k'+G+m+k} \quad 0 \leq k \leq d-1. \tag{11}$$

Similar to the case of $m > 0$, the result of [9] for the case of $m < 0$ and no mobility can be extended to the following for the mobile case:

$$\frac{1}{SIR^l_{mob,ave}} = \frac{N^2}{\sum_{g\in\Theta}\sum_{g'\in\Theta} R_{norm}(g-g')} - 2\frac{\Re\{\sum_{z=0}^{d-1}\sum_{z'=0}^{z+G+m}\sum_{g'\in\Theta}\sigma^2_{z'} R_{norm}(m+z-g')\}}{\sigma^2_H \sum_{g\in\Theta}\sum_{g'\in\Theta} R_{norm}(g-g')} - 1 \tag{12}$$

where $SIR^l_{mob,ave}$ denotes the average Signal to Interference Ratio of a mobile OFDM system for the case of $m < 0$ and $\Theta = \{g' | N+d+m \leq g' \leq N-1 \text{ or } 0 \leq g' \leq N+m-1\}$.

III. Effect of Timing Errors on the Pilot-Aided Channel Estimator for Mobile OFDM

A. Case of $m > 0$

In this section we explore the effect of timing errors on the performance of a pilot-aided channel estimator for mobile OFDM. Consider the case of $m > 0$. By taking the IFFT of $H^r_{mob,eq}$ of Eq. 7, the time-domain equivalent channel will be: $h^r_{mob,eq}(k) = \underbrace{h^{norot,r}_{((k+m))_N}}_{\text{rotation in base } N}$, where $h^{norot,r}$ represents the IFFT of $H^{norot,r}$. As can be seen a timing synchronization error of m sampling periods introduces a rotation of m in the base of N in the equivalent channel. We will next prove that $h^{norot,r}$ has the same delay spread length as h. For $0 \leq k \leq C$,

$$h^{norot,r}(k) = \frac{1}{N}\sum_{i=0}^{N-1} H^{norot,r}(i) e^{\frac{j2\pi ki}{N}} = \frac{1}{N^2}\sum_{i=0}^{N-1} e^{\frac{j2\pi ki}{N}} \sum_{z=0}^{N-1} e^{\frac{-j2\pi mz}{N}} \Gamma^r_z H_{((i-z))_N,N-z} =$$
$$\sum_{z=0}^{N-1} e^{\frac{-j2\pi mz}{N}} \Gamma^r_z \sum_{i=0}^{N-1} e^{\frac{j2\pi ki}{N}} \sum_{g=0}^{C}\sum_{g'=0}^{N-1} \frac{h^{(g')}_g}{N^3} e^{\frac{-j2\pi(gi-g'z)}{N}} =$$
$$\sum_{g'=0}^{N-1} \frac{h^{(g')}_k}{N^2} \sum_{z=0}^{N-1} e^{\frac{j2\pi z(g'-m)}{N}} \Gamma^r_z = \frac{1}{N}\sum_{g'=m}^{N-1} h^{(g')}_k. \tag{13}$$

As can be seen from Eq. 13, $h^{norot,r}$ has the same length as the original channel. Therefore, the rotation introduced by timing errors will result in the expansion of $h^{norot,r}$ beyond its maximum predicted length as was the case in Part I. To see the effect of timing errors on channel estimation analytically, consider the case that L equally-spaced pilot tones are inserted among the sub-carriers. Time-domain estimate of the channel can be achieved by estimation at pilot tones followed by an IFFT of length L and an FFT of length N (see [11] for more details). The time-domain channel estimate can be expressed as follows (see [8] for more details):

$$\hat{h}^r_{mob,eq}(k) = \underbrace{h^{norot,r}_{((k+m))_L}}_{\text{rotation in base } L} + \underbrace{u^{mob,r}_k}_{\text{Interference}} + \underbrace{v^{mob,r}_k}_{\text{AWGN}}, \quad (14)$$

where $u^{mob,r}$ and $v^{mob,r}$ are the IFFTs of $U^{mob,r}_i$ and $V^{mob,r}_i$ respectively:

$$U^{mob,r}_i = \sum_{z=0}^{L-1} \alpha_{i,z} \frac{\frac{\Gamma^r_0}{N} e^{\frac{j2\pi m l_z}{N}} ICI_{mob}(l_z) + I^r_{mob,l_z} + S_{mob,l_z}}{X_{pilot}(l_z)}$$
$$V^{mob,r}_i = \sum_{z=0}^{L-1} \alpha_{i,z} \frac{W^r_{mob,l_z}}{X_{pilot}(l_z)} \quad (15)$$

with $l_z = \frac{N}{L}z$, $\alpha_{i,z} = \frac{1}{L}\sum_{g=0}^{L-1} e^{j2\pi g(\frac{z}{L}-\frac{i}{N})}$ and ICI_{mob}, I^r_{mob} and S_{mob} are as defined for Eq. 7. By comparing $h^r_{mob,eq}$ and $\hat{h}^r_{mob,eq}$, we can see that there are three factors contributing to channel estimation error: effect of rotations in different bases, interference and noise. The first factor is a result of the equivalent channel having a rotation in the base of N while the estimated equivalent channel has a rotation in the base of L, as discussed in details in Part I. This means that there will be a mismatch in the location of the first m paths of $h^{norot,r}$ which can degrade the performance considerably (see Fig. 1 of Part I). High mobility, however, changes the expressions of the interference terms as can be seen by comparing Eq. 15 of this paper with Eq. 18 of Part I. To analytically assess the contribution of each of the aforementioned factors, an expression for the average channel estimation error variance is derived next. We will have for $0 \le i \le N-1$,

$$\Delta H^r_{mob,eq}(i) = \sum_{k=0}^{m-1} \beta^r_{i,k} h^{norot,r}_k + U^{mob,r}_i + V^{mob,r}_i, \quad (16)$$

where $\Delta H^r_{mob,eq}$ represents the frequency-domain channel estimation error for the mobile case and $\beta^r_{i,k} = \frac{N-m}{N} \times e^{\frac{-j2\pi i(k-m)}{N}} \times (1 - e^{-\frac{j2\pi i L}{N}})$.

Theorem 2: Consider a mobile OFDM system with a timing synchronization error of m sampling periods to the right. Let $Ch^{mob,r}_{error,norm}(i)$ represent the normalized average channel estimation error variance of the pilot-aided channel estimator. Then we will have,

$$Ch^{mob,r}_{error,norm}(i) = \frac{\overline{|\Delta H^r_{mob,eq}(i)|^2}}{\overline{|H^r_{mob,eq}(i)|^2}} \approx \underbrace{4\Upsilon^r_{\%}(m) sin^2(\frac{\pi i L}{N})}_{\text{factor\#1:rotations in different bases}} + \underbrace{\frac{1}{SIR^r_{mob,ave}(m)}}_{\text{interference}} + \underbrace{\frac{1}{SNR^r_{mob,ave}(m)}}_{\text{noise}}. \quad (17)$$

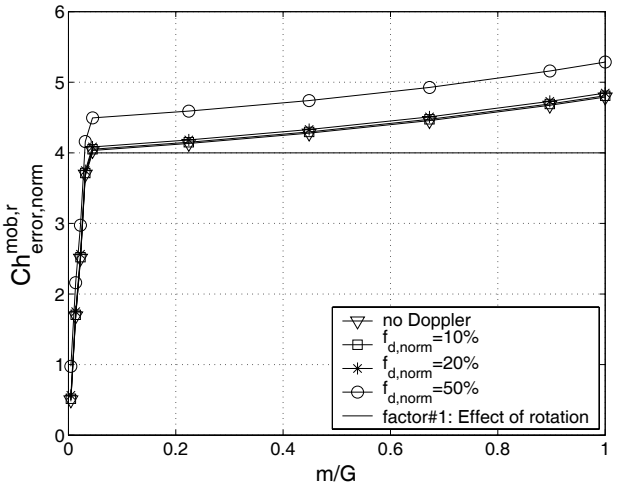

Fig. 1. Normalized channel estimation error variance vs. normalized m (G is the cyclic prefix length), impact of rotations in different bases.

$SIR^r_{mob,ave}(m) = \frac{\sigma^2_X \sigma^2_H \sum_{g'=m}^{N-1}\sum_{g''=m}^{N-1} R_{norm}(g'-g'')}{N^2 |\frac{\Gamma^r_0}{N} e^{\frac{j2\pi m i}{N}} ICI_{mob}(i) + I^r_{mob,i} + S_{mob,i}|^2}$ is analytically evaluated in Theorem 1, $SNR^r_{mob,ave}(m) = \frac{\sigma^2_X \sigma^2_H \sum_{g'=m}^{N-1}\sum_{g''=m}^{N-1} R_{norm}(g'-g'')}{N^2 \sigma^2_W}$, $\overline{X_i X^*_j} = \sigma^2_X \delta_{ij}$ and $\Upsilon^r_{\%}(m) = \frac{\sum_{k=0}^{m-1} \sigma^2_{h_k}}{\sum_{k=0}^{C} \sigma^2_{h_k}}$.

Proof: First $\overline{U^{mob,r}_i h^{*norot,r}_k}$ is calculated. It can be easily shown that $\overline{\left[\frac{ICI_{mob}(l_z) h^{*norot,r}_k}{X_{pilot}(l_z)}\right]} = 0$ and $\overline{\left[\frac{I^r_{mob,l_z} h^{*norot,r}_k}{X_{pilot}(l_z)}\right]} = 0$. Therefore, $\overline{U^{mob,r}_i h^{*norot,r}_k} = \sum_{z=0}^{L-1} \alpha_{i,z} \overline{\left[\frac{S_{mob,l_z} h^{*norot,r}_k}{X_{pilot}(l_z)}\right]} = \frac{1}{N}\sum_{g=m}^{N-1}\sum_{k'=0}^{m-1}\sum_{k''=k'+1}^{C} \overline{h^{(N-m+k')}_{k''} h^{(g)*}_k} \times \sum_{z=0}^{L-1} \alpha_{i,z} \overline{\left[\frac{x_{N-k''+k'}}{X_{pilot}(l_z)}\right]} e^{-\frac{j2\pi(k'-m)z}{L}} = \frac{1}{N^2}\sum_{g=m}^{N-1}\sum_{k'=0}^{m-1}\sum_{k''=k'+1}^{C} \overline{h^{(N-m+k')}_{k''} h^{(g)*}_k} \times \sum_{z=0}^{L-1} \alpha_{i,z} e^{-\frac{j2\pi(k''-m)z}{L}} = \frac{1}{N^2}\sum_{g=m}^{N-1}\sum_{k'=0,k>k'}^{m-1} R_k(N - m + k' - g)\sum_{z=0}^{L-1} \alpha_{i,z} e^{-\frac{j2\pi(k-m)z}{L}}$. Since we are interested in $\overline{U^{mob,r}_i h^{*norot,r}_k}$ only for $0 \le k \le m-1$, we will have $\overline{U^{mob,r}_i h^{*norot,r}_k} = \frac{1}{N^2}\sum_{g=m}^{N-1}\sum_{k'=0}^{k-1} \sigma^2_{h_k} R_{norm}(N - m + k' - g) e^{-\frac{j2\pi(L+k-m)i}{N}}$ for $1 \le k \le m-1$ and $\sum_{k=0}^{m-1} \beta^{*mob}_{i,k} \overline{U^{mob,r}_i h^{*norot,r}_k} = \frac{e^{-\frac{j2\pi Li}{N}}-1}{N^2}\sum_{k=1}^{m-1} \sigma^2_{h_k}\sum_{g=m}^{N-1}\sum_{k'=0}^{k-1} R_{norm}(N-m+k'-g)$ for $m \ge 2$. Similar to the derivation of Part I, it can be easily shown that[2] $E\left[\frac{I^r_{mob,l_z} \times I^{r*}_{mob,l_{z'}}}{X_{pilot}(l_z) X^*_{pilot}(l_{z'})}\right] = 0$, $E\left[\frac{ICI_{mob}(l_z) \times ICI^*_{mob}(l_{z'})}{X_{pilot}(l_z) X^*_{pilot}(l_{z'})}\right] = 0$, $E\left[\frac{I^r_{mob,l_z} \times ICI^*_{mob}(l_{z'})}{X_{pilot}(l_z) X^*_{pilot}(l_{z'})}\right] = 0$, $E\left[\frac{ICI_{mob}(l_z) \times S^*_{mob,l_{z'}}}{X_{pilot}(l_z) X^*_{pilot}(l_{z'})}\right] = 0$ and $E\left[\frac{I^r_{mob,l_z} \times S^*_{mob,l_{z'}}}{X_{pilot}(l_z) X^*_{pilot}(l_{z'})}\right] = 0$ for $z \ne z'$. For an arbitrary

[2]These terms will result in $E\left[\frac{X_g X^*_{g'}}{X_k X^*_{k'}}\right]$ for arbitrary g, g', k and k' where $k \ne k'$, $g \ne k$ and $g' \ne k'$. It can be verified that for non PAM modulations, $E\left[\frac{X_g X^*_{g'}}{X_k X^*_{k'}}\right] = 0$. See Part I for more details.

n and n' where $n \neq n'$, we have $E\left[\frac{S_{mob,n}S^*_{mob,n'}}{X_n X^*_{n'}}\right] = \sum_{k=0}^{m-1}\sum_{g=0}^{m-1}\sum_{k'=max(k,g)+1}^{C} \frac{\sigma^2_{h_{k'}} R_{norm}(k-g)}{N^2} e^{-\frac{j2\pi(k'-m)(n-n')}{N}}$. Therefore, $\sum_{z=0}^{L-1}\sum_{z'=0,z'\neq z}^{L-1} \alpha_{i,z}\alpha^*_{i,z'} E\left[\frac{S_{mob,l_z}S^*_{mob,l_{z'}}}{X_{pilot}(l_z)X^*_{pilot}(l_{z'})}\right] = \sum_{k=0}^{m-1}\sum_{g=0}^{m-1}\sum_{k'=max(k,g)+1}^{C} \frac{\sigma^2_{h_{k'}} R_{norm}(k-g)}{N^2L^2} \sum_{n=0}^{L-1}\sum_{n'=0}^{L-1} e^{-\frac{j2\pi i(n-n')}{N}} \times [\sum_{z=0}^{L-1} e^{\frac{j2\pi z(n-k'+m)}{L}} \sum_{z'=0}^{L-1} e^{-\frac{j2\pi z'(n'-k'+m)}{L}} - \sum_{z=0}^{L-1} e^{\frac{j2\pi z(n-n')}{L}}]$. It can be confirmed (similar to the derivation of Part I) that

$$\sum_{z=0}^{L-1}\sum_{z'=0,z'\neq z}^{L-1} \alpha_{i,z}\alpha^*_{i,z'} E\left[\frac{S_{mob,l_z}S^*_{mob,l_{z'}}}{X_{pilot}(l_z)X^*_{pilot}(l_{z'})}\right] = 0. \quad (18)$$

Therefore, $\sigma^2_{U_i^{mob,r}} = \sum_{z=0}^{L-1} |\alpha_{i,z}|^2 \frac{|\frac{\Gamma^r_0}{N} e^{\frac{j2\pi mz}{L}} ICI_{mob}(l_z) + I^r_{mob,l_z} + S_{mob,l_z}|^2}{\sigma^2_X}$ and

$$\overline{|\Delta H^r_{mob,eq}(i)|^2} = \sum_{k=0}^{m-1} |\beta^{mob}_{i,k}|^2 \sigma^2_{h_k^{norot,r}} + \sigma^2_{U_i^{mob,r}} + \sigma^2_{V_i^{mob,r}} + 2\Re\{\sum_{k=0}^{m-1} \beta^{mob*}_{i,k} \underbrace{U_i^{mob,r} h_k^{*norot,r}}\}, \quad (19)$$

where $\Re\{.\}$ represents the real part of the argument. Using Eq. 13,

$$\overline{|H^{norot,r}(k)|^2} = \frac{\sigma^2_H}{N^2} \sum_{g'=m}^{N-1}\sum_{g''=m}^{N-1} R_{norm}(g'-g''). \quad (20)$$

Similar to the derivation of the estimation error variance in Part I, it can be verified that the last term of Eq. 19 is considerably smaller than the rest of the terms, which results in Eq. 17. ■

Comparing this with the no mobility case of Part I, it can be seen that rotations in different bases have the same contribution as they had in the low-mobility case (see Eq. 38 of Part I). However, the second and third terms on the right hand side of Eq. 17 have slightly higher values compared to their corresponding terms in the low-mobility case. Still rotations in different bases will be the main contributor to the estimation error even for high levels of mobility.

Fig. 1 shows $Ch^{mob,r}_{error,norm}$ for those sub-carriers at mid-points between every two consecutive pilot tones and for different levels of mobility. The following power-delay profile is used for this example: [0.1214 0.1969 0.0987 0.0784 0.1242 0.1969 0.0987 0.0623 0.0197]. $f_{d,norm}$ refers to the maximum Doppler spread divided by the sub-carrier spacing and each channel path has Jakes power spectrum [6]. To see the contribution of the rotation factor, the solid line shows the contribution of the first term on the right-hand side of Eq. 17. Consider the case of no Doppler first. It can be seen that *factor#1* contributes almost all the channel estimation error at low m. As m approaches the length of the guard interval, G, ICI and ISI introduced by timing synchronization errors increase. Still, *factor#1* contributes to more than 80% of the channel estimation error at $m = G$ for the no Doppler case. Comparing the channel estimation error variance of the mobile cases to that of the no Doppler scenario shows that mobility has a negligible impact on channel estimation error, in the presence of timing errors, for $f_{d,norm}$ as high as 20%. This is due to the fact that the effect of rotation is considerably high. To examine a case where Doppler has a non-negligible impact on channel estimation error, $f_{d,norm}$ is increased to 50%. Even for such a high Doppler spread, Fig. 1 shows that *factor#1* contributes to more than 70% of channel estimation error. The timing synchronization method proposed in Part I is effective as long as *factor#1* is the major contributor to the channel estimation error. The analysis of this section showed that in the presence of timing errors, mobility has a negligible impact on channel estimation. Therefore, extending the method proposed in Part I will also provide a robust timing synchronization for high-mobility applications as we shall see later in this paper.

B. Case of $m < 0$

Similar expressions can be derived for the case of $m < 0$: $h^l_{mob,eq}(k) = \underbrace{h^{norot,l}_{((k+m))_N}}_{\text{rotation in base } N}$ and $h^{norot,l}(k) = \frac{1}{N}\sum_{g'\in\Theta} h^{(g')}_k$, where Θ is as defined in Eq. 12. Since the length of $h^{norot,l}$ is the same as the length of the original channel delay spread, rotation will have the same impact as it had for low-mobility cases in Part I. Following a procedure similar to the $m > 0$ case, the following expressions can be derived:

$$\hat{h}^l_{mob,eq}(k) = \overbrace{h^{norot,l}_{((k+m))_L}}^{\text{rotation in base } L} + \overbrace{u^{mob,l}_k}^{\text{Interference}} + \overbrace{v^{mob,l}_k}^{\text{AWGN}}, \quad (21)$$

$$\Delta H^l_{mob,eq}(i) = \sum_{k=0}^{m-1} \beta^{mob}_{i,k} h^{norot,l}_k + U^{mob,l}_i + V^{mob,l}_i \quad (22)$$

for $0 \leq i \leq N-1$ and

$$Ch^{mob,l}_{error,norm}(i) = \frac{\overline{|\Delta H^l_{mob,eq}(i)|^2}}{|H^l_{mob,eq}(i)|^2} \approx \underbrace{4\Upsilon^l_{\%}(m) sin^2(\frac{\pi i L}{N})}_{\text{factor\#1:rotations in different bases}} + \underbrace{\frac{1}{SIR^l_{mob,ave}(m)}}_{\text{interference}} + \underbrace{\frac{1}{SNR^l_{mob,ave}(m)}}_{\text{noise}}, \quad (23)$$

where $SIR^l_{mob,ave}(m)$ is defined in Section II, $\Upsilon^l_{\%}(m) = \frac{\sum_{k=L+m}^{L-1}\sigma^2_{h_k}}{\sum_{k=0}^{C}\sigma^2_{h_k}}$ and $SNR^l_{mob,ave}(m) = \frac{\sigma^2_X\sigma^2_H\sum_{g'\in\Theta}\sum_{g''\in\Theta} R_{norm}(g'-g'')}{N^2\sigma^2_W}$. It can be seen that effect of rotations in different bases is the same as before. Mobility can result in a slight increase of the second and third terms on the right hand side of Eq. 23. Similar to the low-mobility case, errors to the left may not degrade the performance depending on the length of the channel delay spread, length of the guard interval and number of pilot tones.

IV. Timing Synchronization Error Correction

In Part I, we utilized the super-sensitivity of the pilot-aided channel estimator to timing errors (specifically rotations in different bases) to design a robust timing synchronization algorithm. This paper showed that effect of rotation is still the main contributor to channel estimation error even in high-mobility cases. Therefore, this sensitivity can still be used to design a synchronization algorithm that works robustly in high-mobility

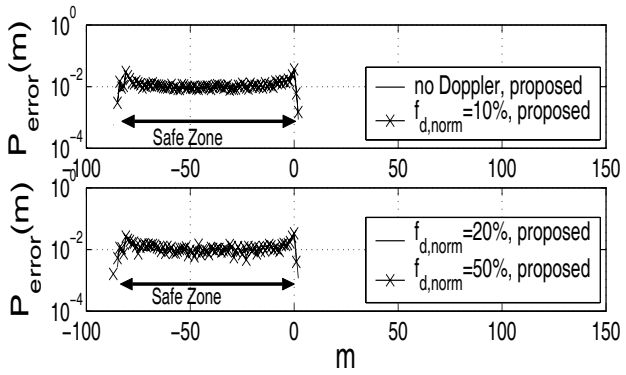

Fig. 2. Performance of the proposed synchronizer for channel#1 and $\frac{\sigma_X^2\sigma_H^2}{\sigma_W^2} = 20dB$, high-mobility cases.

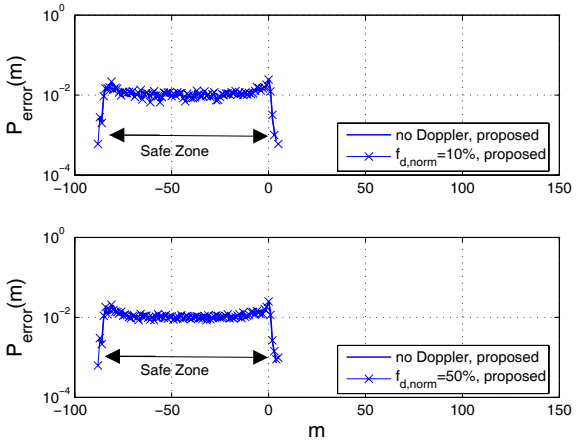

Fig. 3. Performance of the proposed synchronizer for channel#1 and $\frac{\sigma_X^2\sigma_H^2}{\sigma_W^2} = 10dB$, high-mobility cases.

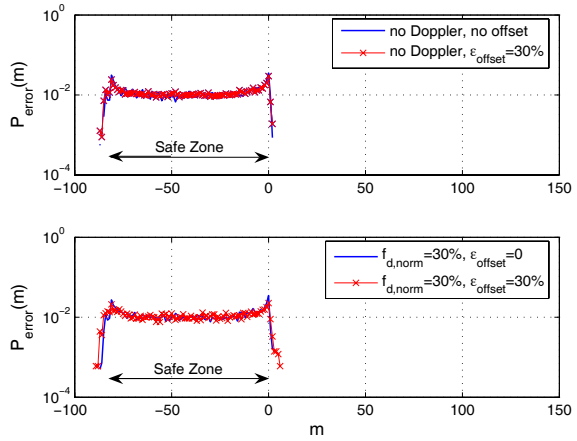

Fig. 4. Performance of the proposed synchronizer for channel#1, in the presence of a frequency offset and for high mobility cases, $\frac{\sigma_X^2\sigma_H^2}{\sigma_W^2} = 20dB$

environments, without a need for synchronization training overhead. After a coarse timing synchronizer has detected a start point for the OFDM symbol (a correlation-based synchronizer can be used for this as discussed in Part I), $\hat{H}_{mob,eq}$ can be obtained using pilot tones. In the presence of timing errors, this channel estimate may be considerably different from $H_{mob,eq}$. Let $\hat{X}_i = \frac{Y_{mob,i}}{\hat{H}_{mob,eq}(i)}$ and $\tilde{X}_i = Dec(\hat{X}_i)$ represent the estimated input at the i^{th} sub-channel before and after the decision device respectively. Define a decision-directed measure function as follows: $MF = \sum_{i=0}^{N-1} |\hat{X}_i - \tilde{X}_i|^2$. MF can become considerably high due to the impact of channel rotation. Therefore, timing synchronization error correction can be achieved by minimizing MF. As long as *factor#1* is the major cause of performance loss, which is the case with high probability, timing errors can be detected. Through an iterative process, the estimated channel is updated, correcting for one mismatched path at a time. Following the procedure described in Part I, the update necessary for correcting errors to the right at the i^{th} iteration and k^{th} sub-channel will be as follows:

$$\hat{H}_{mob,eq}^{(i+1),r}(k) = \hat{H}_{mob,eq}^{(i),r}(k) + \varsigma \times \hat{h}_{mob,eq}^{r}(L-k) \times e^{\frac{j2\pi ik}{N}}. \quad (24)$$

Similarly,

$$\hat{H}_{mob,eq}^{(i+1),l}(k) = \hat{H}_{mob,eq}^{(i),l}(k) - \varsigma \times \hat{h}_{mob,eq}^{l}(i-1) \times e^{-j2\pi(i-1)k/N}, \quad (25)$$

where $\varsigma = 1 - e^{-\frac{j2\pi Lk}{N}}$ and $\hat{H}_{mob,eq}^{(1),r}(k) = \hat{H}_{mob,eq}^{(1),l}(k) = \hat{H}_{mob,eq}(k)$. In each iteration, the measure function, $MF^{(i)}$, will be evaluated. Finally the iteration that minimizes MF is selected and the correction necessary is applied to the start of the symbol in the time domain.

V. Simulation Results

An OFDM system is simulated in a high delay and Doppler spread environment for an SFN channel. System parameters are the same as in Section VI of Part I and are briefly summarized here. Input modulation is 8PSK. Useful bit rate is 7.3Mbps. N=892, $L = G$=223 and $T_s = .26\mu s$. We use channel#1 of Part I, whose power-delay profile has two main clusters each with 9 non-zero paths, to represent an SFN channel. Power-delay profile of Channel#1 is shown in Fig. 3 of Part I and has delay spread of $36.5\mu s$, spanning 64% of the guard interval. The power-delay profile delays are as follows: $[0 \quad 0.2568 \quad 0.5136 \quad 1.0273 \quad 1.2841 \quad 1.5409 \quad 2.0545 \quad 2.3113 \quad 3.0818 \quad 33.3818 \quad 33.6386 \quad 33.8954 \quad 34.4091 \quad 34.6659 \quad 34.9227 \quad 35.4363 \quad 35.6931 \quad 36.5]\mu s$. Each channel path is generated as a random process with Rayleigh distributed amplitude and uniformly distributed phase using Jakes Doppler spectrum [6]. Therefore, the time-domain autocorrelation of each channel path is a zero-order Bessel function. Figs. 4 and 5 of Part I showed the performance of the proposed algorithm for low-mobility cases. Fig. 3 of this paper shows similar curves for different levels of mobility: $f_{d,norm}$ =10%, 20% and 50% and at $SNR = 20dB$. $P_{error}(m)$ denotes the average probability that the timing synchronizer makes an error of m sampling periods. Compared with the no Doppler case, it can be observed that the error profile is not affected by high mobility and that the proposed synchronizer still mainly makes error in the "*safe zone*". "*safe zone*" denotes the region where there is no cost for making a timing error due to the presence of the cyclic prefix, as explained in Part I. To see the performance

in lower SNR cases, Fig. 3 shows the performance at $SNR = 10dB$. It can be seen that the performance of the proposed timing synchronizer is still very close to the no Doppler case. The robust performance of the synchronizer is due to the considerable impact of *factor#1* on the channel estimation error as was confirmed in the previous sections. This shows that the proposed algorithm can be utilized for robust timing synchronization in high delay and Doppler spread environments, without a need for synchronization training overhead.

VI. Performance of the Proposed Timing Synchronizer in the Presence of a Frequency Offset

In this section we will show how mathematical framework of the previous sections can be extended for timing synchronization in the presence of a frequency offset. Frequency offset can be viewed as time-variations in the channel making mathematical analysis of the previous sections applicable. Consider a case where there is some residual frequency offset in the receiver, Δ_{offset}. First consider a case where there is no mobility, i.e. channel is constant over an OFDM symbol. Let ϑ_i^o represent the time-domain channel output for the case of perfect synchronization, in the absence of mobility, and in the presence of Δ_{offset}. We will have, $\vartheta_i^o = \sum_{k=0}^{G} h_k x_{((i-k))_N} e^{j2\pi\epsilon i/N}$ for $0 \leq i \leq N-1$, where $\epsilon = \frac{\Delta_{offset}}{\Delta_f}$ with Δ_f representing the sub-carrier spacing. Comparing this with Eq. 1 shows that this case can be looked at as a time-varying channel case with the following equivalent channel paths: $h_k^{(i),offset} = h_k e^{j2\pi\epsilon i/N}$. This results in the following auto-correlation characteristics: $R_g^{offset}(z) = \sigma_g^2 e^{j2\pi\epsilon z/N}$ and $R_{g,norm}^{offset}(z) = e^{j2\pi\epsilon z/N}$. Using these equations, the rest of the derivations will be all applicable. For instance Eq. 8 and 12 can be used to measure SIR in the presence of both timing errors and frequency offset. Furthermore, Eq. 17 and 23 can be used to show the impact of timing errors on channel estimation in the presence of a frequency offset.

For mobile cases, where channel is time-varying within one OFDM symbol, the impact of a frequency offset can be included in the channel modeling as follows: $h_k^{(i),o,d} = h_k^{(i)} e^{j2\pi\epsilon i/N}$, where $h_k^{(i),o,d}$ refers to the equivalent channel paths in the presence of both a frequency offset and mobility (no timing errors yet). Then channel auto-correlation characteristics will be as follows: $R_g^{o,d}(z) = R_g(z) e^{j2\pi\epsilon z/N}$ and $R_{g,norm}^{o,d}(z) = R_{g,norm}(z) e^{j2\pi\epsilon z/N}$, where $R_g^{o,d}(z)$ and $R_{g,norm}^{o,d}(z)$ represent the auto-correlation and the normalized auto-correlation of the g^{th} equivalent channel path in the presence of both Doppler and a frequency offset respectively and $R_g(z)$ and $R_{g,norm}(z)$ are as defined in Section II for the mobile case. Then the rest of the analysis can be used to characterize the impact of timing errors on channel estimation for high mobility cases and in the presence of a frequency offset. Furthermore, the proposed algorithm can be utilized for timing synchronization for high mobility cases and in the presence of a frequency offset. To see the performance of the proposed algorithm for high mobility cases and in the presence of a frequency offset, Fig. 4 shows $P_{error}(m)$ as a function of timing offset and for different levels of mobility and frequency offsets. System parameters and power-delay profile are the same as those used in Section V. It can be seen that the proposed algorithm works robustly for a high delay spread fading channel in the presence of both Doppler spreads and frequency offsets. As both Doppler spread and frequency offset increase, it can be seen that error probability increases slightly (bottom figure). Nevertheless, the timing synchronizer has a robust performance and still makes errors mainly in the *"safe zone"*.

VII. Summary

In this paper we first characterized the impact of both mobility and timing synchronization errors on the performance of a pilot-aided OFDM system. More specifically, we found analytical expressions for the average Signal to Interference Ratio and average channel estimation error variance of a mobile OFDM system in the presence of timing errors and for a frequency-selective fading channel. The results indicated that a pilot-aided channel esitmator is considerably sensitive to timing errors, due to the impact of rotations in different bases, even for high levels of mobility. Based on the analysis, we extended the timing synchronization algorithm proposed for low-mobility applications in Part I to high-mobility cases. Our analysis and simulation results showed that the proposed synchronizer works robustly in high delay and Doppler spread environments, without relying on training information. Finally, we showed how our mathematical framework and proposed algorithm can be utilized for robust timing synchronization in the presence of both a Doppler spread and a frequency offset.

VIII. Appendix

Proof of Theorem 1

The power of the second term on the right hand side of Eq. 7 will be as follows:

$$\begin{aligned} E(|\tfrac{\Gamma_0^r}{N} e^{\frac{j2\pi mi}{N}} ICI_{mob}(i)|^2) &= \tfrac{|\Gamma_0^r|^2}{N^2} E(|ICI_{mob}(i)|^2) \\ &= \tfrac{(N-m)^2\sigma_X^2}{N^2} \textstyle\sum_{z=1}^{N-1} \overline{|H_{i,z}|^2} \\ = \tfrac{(N-m)^2\sigma_X^2\sigma_H^2}{N^4} (N^2 - \textstyle\sum_{g=0}^{N-1}\sum_{g'=0}^{N-1} R_{norm}(g-g')). \end{aligned} \tag{26}$$

Next the average power of $I_{mob,i}^r$ is derived: $\sigma_{I_{mob}^r}^2 = \underbrace{\sum_{k=1}^{N-1}\sum_{k'=0}^{N-1}}_{k+k'\neq N} \underbrace{\sum_{k''=1}^{N-1}\sum_{k'''=0}^{N-1}}_{k''+k'''\neq N} \frac{\sigma_X^2 \Gamma_k^r \Gamma_{k''}^{r*}}{N^2} \overline{H_{((i-k))_N,k'} H^*_{((i-k''))_N,k'''}} e^{-j\frac{2\pi m(k-k'')}{N}}$,

for $k+k' = k''+k'''$ or $k+k' = k''+k'''+N$ or $k+k'+N = k''+k'''$. For arbitrary z, z', n and n', $\overline{H_{z,z'} H^*_{n,n'}} = \sum_{g=0}^{N-1}\sum_{g'=0}^{N-1}\sum_{g''=0}^{N-1} \frac{R_g(g'-g'')}{N^2} e^{-\frac{j2\pi(z'(g'-g)+gz-n'(g''-g)-gn)}{N}}$ $= \frac{1}{N^2}\sum_{g'=0}^{N-1}\sum_{g''=0}^{N-1} R_{norm}(g'-g'') \times \sum_{g=0}^{C} \sigma_g^2 e^{-\frac{j2\pi(g(z-z'+n'-n)+z'g'-n'g'')}{N}}$. Therefore for

$k+k' = k''+k'''$, $k+k' = k''+k'''+N$ or $k+k'+N = k''+k'''$, we will have

$$\overline{H_{((i-k))_N,k'}H^*_{((i-k''))_N,k'''}} = \frac{\sigma_H^2}{N^2}\sum_{g'=0}^{N-1}\sum_{g''=0}^{N-1} R_{norm}(g'-g'')e^{-\frac{j2\pi(k'g'-k'''g'')}{N}}. \quad (27)$$

To have $k+k' = k''+k'''$, for every k and k' there should exist a k'' such that $0 \le k''' = k+k'-k'' \le N-1$. This means that there should exist a k'' in the range of $k+k'-N+1 \le k'' \le k+k'$. Furthermore, if $k+k' \neq N$, then $k''+k''' \neq N$ for this case. To have $k+k' = k''+k'''+N$, for every k and k', there should exist a k'' such that $k+k'-2N+1 \le k'' \le k+k'-N$. In this scenario $k''+k'''$ can not be N. To have $k+k'+N = k''+k'''$, for every k and k', there should exist a k'' such that $k+k'+1 \le k'' \le k+k'+N$. Similarly, $k+k'$ can not be N in this case. Therefore since $k+k'-2N+1 < 1$ and $k+k'+N > N-1$, for every k and k', there always exists a pair of k'' and k''' that satisfies the conditions of Eq. 27. Therefore, $\sigma^2_{I^r_{mob}} = \frac{\sigma_X^2\sigma_H^2}{N^4}\underbrace{\sum_{k=1}^{N-1}\sum_{k'=0}^{N-1}}_{k+k'\neq N}\sum_{k''=1}^{N-1}\Gamma^r_k\Gamma^{r*}_{k''}\sum_{g'=0}^{N-1}\sum_{g''=0}^{N-1} R_{norm}(g'-g'')e^{-\frac{j2\pi(k'g'-(k+k'-k'')g'')}{N}}e^{-j\frac{2\pi m(k-k'')}{N}} = \frac{\sigma_X^2\sigma_H^2}{N^4}\sum_{k=1}^{N-1}\sum_{k''=1}^{N-1}\Gamma^r_k\Gamma^{r*}_{k''}\sum_{g'=0}^{N-1}\sum_{g''=0}^{N-1} R_{norm}(g'-g'') \times \sum_{k'=0}^{N-1} e^{-j\frac{2\pi k'(g'-g'')}{N}}e^{j\frac{2\pi g''(k-k'')}{N}}e^{-j\frac{2\pi m(k-k'')}{N}} - \frac{\sigma_X^2\sigma_H^2}{N^4}\sum_{k=1}^{N-1}\sum_{k''=1}^{N-1}\Gamma^r_k\Gamma^{r*}_{k''}\sum_{g'=0}^{N-1}\sum_{g''=0}^{N-1} R_{norm}(g'-g'') \times e^{\frac{-j2\pi(-kg'+g''k'')}{N}}e^{-j\frac{2\pi m(k-k'')}{N}}$. We will then have,

$$\begin{aligned}\sigma^2_{I^r_{mob}} &= \frac{\sigma_X^2\sigma_H^2}{N^2}\sum_{k=1}^{N-1}|\Gamma_k|^2 - \\ &\frac{\sigma_X^2\sigma_H^2\Gamma_0^2}{N^4}\sum_{g'=0}^{N-1}\sum_{g''=0}^{N-1} R_{norm}(g'-g'') - \\ &\frac{\sigma_X^2\sigma_H^2}{N^2}\sum_{g'=m}^{N-1}\sum_{g''=m}^{N-1} R_{norm}(g'-g'') + \\ &2\frac{\sigma_X^2\sigma_H^2(N-m)}{N^3}\sum_{g'=m}^{N-1}\sum_{g''=0}^{N-1}\Re\{R_{norm}(g'-g'')\},\end{aligned} \quad (28)$$

where $\Re\{.\}$ indicates the real part of the argument. Next the power of $S_{mob,i}$ is calculated. $S_{mob,i} = \sum_{k=0}^{m-1} s_{mob,N-m+k}e^{-\frac{j2\pi i(k-m)}{N}}$, where $s_{mob,N-m+k}$ can be written as follows for $0 \le k \le m-1$:

$$s_{mob,N-m+k} = y^{next}_{mob,pf}(k) = \overbrace{\sum_{k'=k+1}^{C} h^{(N-m+k)}_{k'}x_{N-k'+k}}^{\text{ICI}} + \overbrace{\sum_{k'=0}^{k} h^{(N-m+k)}_{k'}x^{next}_{N-G+k-k'}}^{\text{ISI}}. \quad (29)$$

Similar to the low-mobility case, we will have $\sigma^2_{S_{mob}} = \frac{m\sigma_X^2\sigma_H^2}{N}$. Next, $E[\frac{\Gamma^r_0}{N}e^{\frac{j2\pi mi}{N}}ICI_{mob}(i)S^*_{mob,i}] = \frac{\sigma_X^2\Gamma^r_0}{N^2}\times \sum_{z=1}^{N-1}\sum_{k=0}^{m-1}\sum_{k'=k+1}^{C}\overline{h^{*(N-m+k)}_{k'}H_{i,z}}e^{-\frac{j2\pi((k-k')(i-z)-ik)}{N}}$.

Since $E[h^{*(N-m+k)}_{k'}H_{i,z}] = \frac{1}{N}\sum_{g'=0}^{N-1}R^*_{k'}(N-m+k-g')e^{-\frac{j2\pi(z(g'-k')+k'i)}{N}}$, then

$$\begin{aligned}&\overline{\frac{\Gamma^r_0}{N}e^{\frac{j2\pi mi}{N}}ICI_{mob}(i)S^*_{mob,i}} = \\ &\frac{\sigma_X^2\Gamma^r_0}{N^2}\sum_{g'=0}^{m-1}\sum_{k'=g'+1}^{C}\sigma^2_{k'}R^*_{norm}(N-m) - \\ &\frac{\sigma_X^2\Gamma^r_0}{N^3}\sum_{g'=0}^{N-1}\sum_{k=0}^{m-1}\sum_{k'=k+1}^{C}\sigma^2_{k'}R^*_{norm}(N-m+k-g').\end{aligned} \quad (30)$$

After a long derivation, it can be shown that,

$$\begin{aligned}&\overline{I^r_{mob,i}S^*_{mob,i}} = \\ &-\frac{\sigma_X^2\Gamma^r_0}{N^2}\sum_{z=0}^{m-1}\sum_{z'=z+1}^{C}\sigma^2_{z'}R^*_{norm}(N-m) + \\ &\frac{\sigma_X^2\Gamma^r_0}{N^3}\sum_{z=0}^{m-1}\sum_{z'=z+1}^{C}\sum_{g'=0}^{N-1}\sigma^2_{z'}R^*_{norm}(N-m+z-g') - \\ &\frac{\sigma_X^2}{N^2}\sum_{z=0}^{m-1}\sum_{z'=z+1}^{C}\sigma^2_{z'}\sum_{g'=m}^{N-1}R^*_{norm}(N-m+z-g').\end{aligned} \quad (31)$$

Therefore,

$$\begin{aligned}&\overline{I^r_{mob,i}S^*_{mob,i} + \frac{\Gamma^r_0}{N}e^{\frac{j2\pi mi}{N}}ICI_{mob}(i)S^*_{mob,i}} = \\ &-\frac{\sigma_X^2}{N^2}\sum_{z=0}^{m-1}\sum_{z'=z+1}^{C}\sigma^2_{z'}\sum_{g'=m}^{N-1}R^*_{norm}(N-m+z-g').\end{aligned} \quad (32)$$

Finally $\overline{\frac{\Gamma^r_0}{N}e^{-\frac{j2\pi mi}{N}}ICI^*_{mob}(i)I^r_{mob,i}}$ is calculated:

$$\begin{aligned}&\overline{\frac{\Gamma^r_0}{N}e^{-\frac{j2\pi mi}{N}}ICI^*_{mob}(i)I^r_{mob,i}} = \frac{\Gamma^r_0}{N^2}\sum_{z=1}^{N-1} \\ &\underbrace{\sum_{k=1}^{N-1}\sum_{k'=0}^{N-1}}_{k+k'\neq N}\Gamma^r_k\overline{H_{((i-k))_N,k'}H^*_{i,z}X_{((i-k-k'))_N}X^*_{((i-z))_N}}e^{-\frac{j2\pi mk}{N}}\end{aligned} \quad (33)$$

Eq. 33 has non-zero values for $k+k' = z$ or $k+k' = N+z$. In both cases, $k+k'$ can not be N. Therefore,

$$\begin{aligned}&\overline{\frac{\Gamma^r_0}{N}e^{-\frac{j2\pi mi}{N}}ICI^*_{mob}(i)I^r_{mob,i}} = \\ &\frac{\Gamma^r_0\sigma_X^2\sigma_H^2}{N^4}\sum_{z=1}^{N-1}\sum_{k=1}^{N-1}\sum_{k'=0}^{N-1}\Gamma^r_k e^{-\frac{j2\pi mk}{N}} \\ &\sum_{g'=0}^{N-1}\sum_{g''=0}^{N-1} R_{norm}(g'-g'')e^{-\frac{j2\pi(k'g'-zg'')}{N}} \\ &\text{for} \quad k+k' = z \quad \text{or} \quad k+k' = N+z.\end{aligned} \quad (34)$$

Then it can be confirmed that $\overline{\frac{\Gamma^r_0}{N}e^{-\frac{j2\pi mi}{N}}ICI^*_{mob}(i)I^r_{mob,i}} = \frac{\Gamma^r_0\sigma_X^2\sigma_H^2}{N^4}\times\sum_{k=1}^{N-1}\Gamma^r_k e^{-\frac{j2\pi mk}{N}}\sum_{g'=0}^{N-1}\sum_{g''=0}^{N-1}R_{norm}(g'-g'') \sum_{k'=0}^{N-1-k}e^{-\frac{j2\pi k'(g'-g'')}{N}}e^{\frac{j2\pi kg''}{N}} + \frac{\Gamma^r_0\sigma_X^2\sigma_H^2}{N^4}\sum_{k=1}^{N-1}\Gamma^r_k e^{-\frac{j2\pi mk}{N}}\sum_{g'=0}^{N-1}\sum_{g''=0}^{N-1}R_{norm}(g'-g'') \sum_{k'=N+1-k}^{N-1}e^{-\frac{j2\pi k'(g'-g'')}{N}}e^{\frac{j2\pi kg''}{N}} = \frac{\Gamma^{r2}_0\sigma_X^2\sigma_H^2}{N^4}\sum_{g'=0}^{N-1}\sum_{g''=0}^{N-1}R_{norm}(g'-g'') - \frac{\Gamma^r_0\sigma_X^2\sigma_H^2}{N^3}\sum_{g'=m}^{N-1}\sum_{g''=0}^{N-1}R_{norm}(g'-g'')$. Using the derived expressions, Eq. 8 can be easily verified.

REFERENCES

[1] A. R. S. Bahai, B. R. Saltzberg, and M. Ergen, *Multi-Carrier Digital Communications-Theory and Applications of OFDM*, 2nd ed. New York: Springer, 2004

[2] J. Bingham, "Multicarrier modulation for data transmission: An idea whose time has come," *IEEE Commun. Mag.*, vol. 28, no. 5, pp. 5-14, May 1990.

[3] L. Cimini, "Analysis and simulation of a digital mobile channel using orthogonal frequency division multiplexing," *IEEE Trans. Commun.*, vol. 33, pp. 665-675, July 1985.

[4] ETSI EN 302 304, "Digital video broadcasting (DVB); Transmission system for handheld terminals (DVB H)," V1.1.1, June 2004.

[5] B. Le Floch, R. Hallbert-Lasalle, and D. Castellain, "Digital audio broadcasting to mobile receivers," *IEEE Trans. Consumer Electron.*, vol. 35, no. 3, pp. 493-503, Aug. 1989.

[6] W. C. Jakes, *Microwave Mobile Communications*. New York: IEEE Press, 1974.

[7] W. G. Jeon and K. H. Chang, "An equalization technique for orthogonal frequency-division multiplexing systems in time-variant multipath channels," *IEEE Trans. Commun.*, vol. 47, no. 1, Jan. 1999.

[8] Y. Mostofi and D. Cox, "A robust timing synchronization design in OFDM systems-Part I: Low-mobility cases," *IEEE Trans. Commun.*, vol. 6, no. 11, Nov. 2007.

[9] Y. Mostofi and D. Cox, "Mathematical analysis of the impact of timing synchronization errors on the performance of an OFDM system," *IEEE Trans. Commun.*, vol. 54, no. 2, pp. 226-230, Feb. 2006.

[10] Y. Mostofi and D. Cox, "ICI mitigation for pilot-aided OFDM mobile systems," *IEEE Trans. Wireless Commun.*, vol. 4, no. 2, pp. 765-774, Mar. 2005.
[11] R. Negi and J. Cioffi, "Pilot tone selection for channel estimation in a mobile OFDM system," *IEEE Trans. Consumer Electron.*, vol. 44, no. 3, pp. 1122-1128, Aug. 1998.
[12] T. S. Rappaport, *Wireless Communications: Principles and Practice*. Upper Saddle River, NJ: Prentice Hall, 1996.
[13] M. Russell and G. Stuber, "Interchannel interference analysis of OFDM in a mobile environment," in *Proc. VTC*, 1995, pp. 820-824.
[14] H. Sari, G. Karam and J. Janclaude, "Transmission techniques for digital TV broadcasting," *IEEE Commun. Mag.*, vol. 36, pp. 100-109, Feb. 1995.
[15] S. Sung and D. Brady, "Spectral spatial equalization for OFDM in time-varying frequency-selective multipath channels," in *IEEE Workshop Sensor Array Multichannel Signal Processing*, 2000, pp. 434-438.
[16] R. D.J. van Nee and R. Prasad, *OFDM for Wireless Multimedia Communications*. Boston, MA: Artech House, 1998.

Yasamin Mostofi (S'98-M'04) received the B.S. degree in electrical engineering from Sharif University of Technology, Tehran, Iran, in 1997, and the M.S. and Ph.D. degrees from Stanford University, Stanford, CA, in 1999 and 2004, respectively. She is currently an assistant professor at the Department of Electrical and Computer Engineering at the University of New Mexico. Prior to that, she was a postdoctoral scholar at the California Institute of Technology from 2004 to 2006. Her research interests include cooperative sensor networks, mobile communications, control and dynamical systems and signal processing.

Donald C. Cox (S'58-M'61-SM'72-F'79) received the B.S. and M.S. degrees in Electrical Engineering from the University of Nebraska in 1959 and 1960, respectively, and the Ph.D. degree in Electrical Engineering from Stanford University in 1968. He received an Honorary Doctor of Science from the University of Nebraska in 1983.

From 1960 to 1963, Mr. Cox did microwave communications system design at Wright-Patterson AFB, Ohio. From 1963 to 1968 he was at Stanford University doing tunnel diode amplifier design and research on microwave propagation in the troposphere. From 1968 to 1973 his research at Bell Laboratories, Holmdel, New Jersey in mobile radio propagation and on high-capacity mobile radio systems provided important input to early cellular mobile radio system development, and is continuing to contribute to the evolution of digital cellular radio, wireless personal communications systems and cordless telephones. From 1973 to 1983 he was Supervisor of a group at Bell Laboratories that did innovative propagation and system research for millimeter-wave satellite communications. In 1978 he pioneered radio system and propagation research for low-power wireless personal communications systems. At Bell Laboratories in 1983 he organized and became Head of the Radio and Satellite Systems Research Department that became a Division in Bell Communications Research (Bellcore) with the breakup of the Bell System on January 1, 1984. He was Division Manager of that Radio Research Division until it again became a department in 1991. He continued as Executive Director of the Radio Research Department where he championed, led and contributed to research on all aspects of low-power wireless personal communications entitled Universal Digital Portable Communications (UDPC). He was instrumental in evolving the extensive research results into specifications that became the U.S. Standard for the Wireless or Personal Access Communications System (WACS or PACS). In September 1993 he became a Professor of Electrical Engineering and Director of the Center for Telecommunications at Stanford University where he continues to pursue research and teaching of wireless mobile and personal communications. He was appointed Harald Trap Friis Professor of Engineering in 1994.

Dr. Cox was a member of the Administrative Committee of the IEEE Antennas and Propagation Society (1986-88), was an Associate Editor of the IEEE TRANSACTIONS ON ANTENNAS AND PROPAGATION (1983-86), is a member of the National Academy of Engineering, is a member of Commissions B, C and F of USNC/URSI, and was a member of the URSI Intercommission Group on Time Domain Waveform Measurements (1982-84). He was awarded the IEEE 1993 Alexander Grapham Bell Medal "For pioneering and leadership in personal portable communications;" was a co-recipient of the 1983 International Marconi Prize in Electromagnetic Wave Propagation (Italy); received the IEEE 1985 Morris E. Leeds award and the IEEE Third Millennium Medal in 2000; and received the 1983 IEEE Vehicular Technology Society paper of the year award, and the IEEE Communications Society 1992 L. G. Abraham Prize Paper Award and 1990 Communications Magazine Prize Paper Award. He received the Bellcore Fellow Award in 1991. Dr. Cox is a fellow of AAAS and the Radio Club of America. He is author or coauthor of many papers and conference presentations, including many invited and several keynote addresses, and books. He has been granted 15 patents. Dr. Cox is a member of Sigma Xi, Sigma Tau, Eta Kappa Nu and Phi Mu Epsilon, and is a Registered Professional Engineer in Ohio and Nebraska.